Acta Pharmaceutica Sinica B 2017;7(1):65–72

Chinese Pharmaceutical Association
Institute of Materia Medica, Chinese Academy of Medical Sciences

Acta Pharmaceutica Sinica B

www.elsevier.com/locate/apsb
www.sciencedirect.com

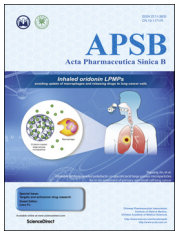

ORIGINAL ARTICLE

Asiatic acid inhibits lung cancer cell growth *in vitro* and *in vivo* by destroying mitochondria

Tiancong Wu[a], Ji Geng[b], Wenjie Guo[c], Jing Gao[b,*], Xixu Zhu[a,*]

[a]*Department of Radiation Oncology, Jinling Hospital, Medical School of Nanjing University, Nanjing 210002, China*
[b]*School of Pharmacy, Jiangsu University, Zhenjiang 212013, China*
[c]*School of Life Science, Nanjing University, Nanjing 210093, China*

Received 12 January 2016; received in revised form 18 February 2016; accepted 9 March 2016

KEY WORDS

Asiatic acid;
Lung cancer;
Apoptosis;
Mitochondria;
Reactive oxygen species

Abstract Asiatic acid (AA), a pentacyclic triterpene found in *Centella asiatica*, displays significant anti-proliferative effects on cancer cells *in vitro* although the underlying mechanism of this effect remains unknown. This study investigated the efficacy and mechanism of action of AA against lung cancer both *in vivo* and *in vitro*. Using the MTT assay, AA was found to induce apoptosis in a dose- and time-dependent manner, an effect enhanced by pretreatment with an autophagy inhibitor. It also elevated expression of microtubule-associated protein 1 light chain 3 (LC3) and decreased the expression of p62. Furthermore, exposure to AA resulted in collapse of the mitochondrial membrane potential and generation of reactive oxygen species (ROS), suggesting mitochondria are the target of AA. In the mouse lung cancer xenograft model, oral administration of AA significantly inhibited tumor volume and weight accompanied by significant apoptosis of lung cancer cells. In addition, it led to a significant decrease in the expression of proliferating cell nuclear antigen (PCNA). In summary, the results show that AA significantly reduces lung cancer cell growth both *in vitro* and *in vivo* and that the associated apoptosis is mediated through mitochondrial damage.

*Corresponding author.
E-mail addresses: guowj@nju.edu.cn (Wenjie Guo), jinggao@ujs.edu.cn (Jing Gao), zhuxixu@hotmail.com (Xixu Zhu).

Peer review under responsibility of Institute of Materia Medica, Chinese Academy of Medical Sciences and Chinese Pharmaceutical Association.

http://dx.doi.org/10.1016/j.apsb.2016.04.003

1. Introduction

Lung cancer is associated with high morbidity and mortality to such an extent that in 2014 it was the leading cause of death among all cancer patients in the United States[1]. In fact, in that year, an estimated 221,200 cases of lung cancer were diagnosed and 158,040 people died from the disease[1]. Although there have been advances in our knowledge of the biology of the disease and treatment options for lung cancer have increased, nevertheless the 5-year relative survival remains low at currently only 18%[1]. In the case of non-small cell lung cancer (NSCLC), drugs targeting epidermal growth factor receptor (EGFR), such as gefitinib and erlotinib[2–6], have been approved but their efficacy is limited and more than 50% of NSCLC patients are not suitable to receive them[5,7]. Therefore, lung cancer remains a public health challenge and novel anticancer drugs are needed.

Asiatic acid (AA) is a triterpene extracted from *Centella asiatica* (L.) Urban (Umbelliferae) that has a long history of successful use in both traditional Chinese and Indian Ayurvedic medicine. Previous studies have demonstrated that AA exhibits a variety of pharmacological effects not only as an antioxidant, antiinflammatory and neuroprotective agent[8–11], but also against cancer. For example, AA induces apoptosis in human SK-MEL-2 melanoma cells by triggering generation of reactive oxygen species (ROS)[12] and does the same thing in HepG2 human hepatoma cells by releasing intracellular Ca^{2+} and enhancing expression of p53[13]. In addition, AA activates extracellular signal-regulated kinase and p38 mitogen-activated protein kinase pathways and induces human breast cancer apoptosis and cell cycle arrest[14]. While these *in vitro* data testify to the anti-cancer efficacy of AA, evidence from *in vivo* studies is limited. How ever, it has been shown to prevent 9,10-dimethylbenz[*a*]anthracene (DMBA)-initiated and 12-*O*-tetradecanoylphorbol-13-acetate (TPA)-promoted mouse skin tumorigenesis by inhibiting NO and COX-2 signaling[15].

In the present study, we evaluated the effects of AA on lung cancer cells *in vitro* and in the mouse Lewis lung cancer xenograft model *in vivo*. As part of the work, we attempted to clarify the mechanism of AA-induced apoptosis and its efficacy against lung cancer

2. Materials and methods

2.1. Materials

Materials (suppliers) were as follows: AA, *N*-acetylcysteine (NAC), chloroquine (CQ) and 3-methyladenine (3-MA, Sigma–Aldrich); 3-[4,5-dimethyl-2-thiazolyl]-2,5-diphenyl-2*H*-tetrazolium bromide (MTT, Amresco); JC-1 (5,5′,6,6′-tetrachloro-1,1′,3,3′-tetraethylbenzimidazolylcarbocyanine iodide), Dulbecco's modified Eagle's medium (DMEM) and Roswell Park Memorial Institute (RPMI)-1640 medium (Life Technology, Waltham, MA, USA); annexin V/propidium iodide (PI) kits for apoptosis, transferase-mediated deoxyuridine triphosphate-biotin nick end labeling (TUNEL) assay kit and DCFH-DA kit (Beyotime Institute of Biotechnology, Nantong, China); antibodies against peroxisome proliferator-activated receptor (PARP), cytochrome c, caspase-3, caspase-9, cytochrome oxidase subunit IV (COXIV), LC3 and p62 (Cell Signaling Technology, Boston, MA, USA); β-actin and proliferating cell nuclear antigen (PCNA, Santa Cruz Biotechnology, Santa Cruz, CA, USA). All other chemicals were of high purity and purchased from commercial sources.

2.2. Cell culture

Human A549 and H1299 lung cancer cell lines and mouse Lewis lung cancer (LLC) cells were purchased from the Shanghai Institute of Cell Biology, Shanghai, China. Cells were maintained in DMEM medium supplemented with 10% (*v*/*v*) heat-inactivated fetal bovine serum and antibiotics (100 U/mL penicillin and 100 U/mL streptomycin) at 37 °C in a humidified atmosphere of 5% CO_2 (Thermo Fisher Scientific, MA, USA).

2.3. Animals

C57BL/6J mice (6–8 weeks old) were purchased from the Shanghai Laboratory Animal Center, Shanghai, China. Briefly, mice were housed in plastic cages at 21 ± 2 °C on a 12 h light–dark cycle with free access to pellet food and water. Animal welfare and experimental procedures were carried out in strict accordance with the Guide for the Care and Use of Laboratory Animals (Ministry of Science and Technology of China, 2006) and related ethical regulations of Nanjing University. All efforts were made to minimize animal suffering and to reduce the number of animals used.

2.4. MTT assay

Cells were plated at a density of approximately 4×10^3 cells/well in 96-well plates and treated with various concentrations of AA in triplicate. After incubation for various times, the MTT assay was applied to determine cell viability using a 96-well plate reader (Spectra MAX 190, Molecular Devices Corporation, CA, USA).

2.5. Cell apoptosis and cell cycle assay

Into 6-well plates 1×10^5 A549 cells were seeded and subsequently treated with AA (20, 40 and 80 mol/L) for up to 24 h. Cells were then stained with 4′,6-diamidino-2-phenylindole (DAPI) and the nuclei photographed. In another experiment, cells were collected, washed with PBS, stained with annexin V/PI in binding buffer at room temperature for 15 min in the dark and then analyzed by fluorescence activated cell sorting (FACS) using a Calibur flow cytometer (Becton Dickinson, NJ, USA). annexin V^+/PI^- and annexin V^+/PI^+ cells were considered to be in the early and late phases of apoptosis. To examine the cell cycle, cells were collected, washed with PBS and then suspended in 1 mL DNA staining solution (20 mg/mL of PI and 100 mg/mL of RnaseA in PBS) for 30 min on ice. DNA content was analyzed by FACS (Becton Dickinson, USA) and the resulting DNA histograms quantified using Cell Quest Pro software.

2.6. Western blot analysis

Proteins were extracted in lysis buffer (30 mmol/L Tris pH 7.5, 150 mmol/L sodium chloride, 1 mmol/L phenylmethylsulfonyl fluoride, 1 mmol/L sodium orthovanadate, 1% Nonidet P-40, 10% glycerol and phosphatase and protease inhibitors), separated by SDS-PAGE and electrophoretically transferred onto polyvinylidene fluoride membranes. The membranes were probed with antibodies overnight at 4 °C and then incubated with a horse radish peroxidase-coupled secondary antibody. Detection was performed using the LumiGLO chemiluminescent substrate system (KPL, Gaithersburg, MD, USA).

2.7. *Mitochondrial membrane potential*

To determine mitochondrial membrane potential, A549 cells were washed with PBS and incubated with 5 μg/mL JC-1 at 37 °C for 30 min. Cells were then washed twice with PBS and immediately examined by fluorescence spectrometry using a fluorescence microplate reader (Spectra MaxGemini, Molecular Devices Corporation, USA). A 488 nm filter was used for excitation of JC-1 and emissions at 535 and 595 nm were used to quantify the population of mitochondria with green (JC-1 monomers) and red (JC-1 aggregates) fluorescence respectively. The red/green ratio was used to reflect the mitochondrial membrane potential.

2.8. *Intracellular ROS*

The intracellular generation of ROS was analyzed using DCFH-DA (2′,7′-dichlorodihydrofluorescein diacetate) as a probe. Cells were incubated with 10 μmol/L DCFH-DA at 37 °C for 15 min. Then DCFH-DA fluorescence distribution of 1×10^4 cells was measured using the fluorescence microplate reader (Spectra MaxGemini, Molecular Devices Corporation, USA) at excitation and emission wavelengths of 488 and 535 nm, respectively.

2.9. *In vivo tumor growth assay*

LLC cells were cultured, collected by centrifugation (1000 rpm, 5 min, Eppendorf 5424R, Hamburg, Germany) and washed twice with ice-cold PBS. They were then diluted to 1×10^7 cells/mL with PBS and 0.1 mL injected subcutaneously into the right flanks of female C57BL6/J mice (6–8 weeks of age). All mice formed tumors 3 days after injection. Mice were subsequently distributed into 4 groups ($n=8$) according to tumor volume and vehicle and AA (50 and 100 mg/kg) administered (i.g.) to each mouse every day from day 0. Tumor length and width were measured with a vernier caliper every 3 days and tumor volume calculated using the equation:

$$\text{Volume} = a \times b^2/2 \quad (1)$$

where a is the maximal width and b is maximal orthogonal length. On the 13th day, mice were weighed, euthanized and the tumors removed and weighed.

2.10. *Immunohistochemistry*

Paraffin-embedded tumor sections were stained with a 1:400 dilution of PCNA primary antibody. Detection was performed using the Real Statistic Analysis Envision Detection kit. The images were collected by microscopy (BX51TRF, Olympus).

2.11. *TUNEL assay*

Paraffin-embedded tumor sections were stained with TUNEL-FITC (1:100) and then counter-stained with DAPI for 5 min. Images were acquired using a Confocal Laser-Scanning Microscope (Olympus FV1000).

2.12. *Statistical analysis*

Comparisons were made by one-way analysis of variance (ANOVA). Differences were considered to be significant when $P<0.05$. All experiments were carried out in triplicate.

3. Results

3.1. *Anti-lung cancer cell growth activity*

AA inhibited A549, H1299 and LLC cell proliferation in both a dose- and time-dependent way (Fig. 1A and C). Photographs of cells (Fig. 1B) shows that, compared to the adherent and spindle-

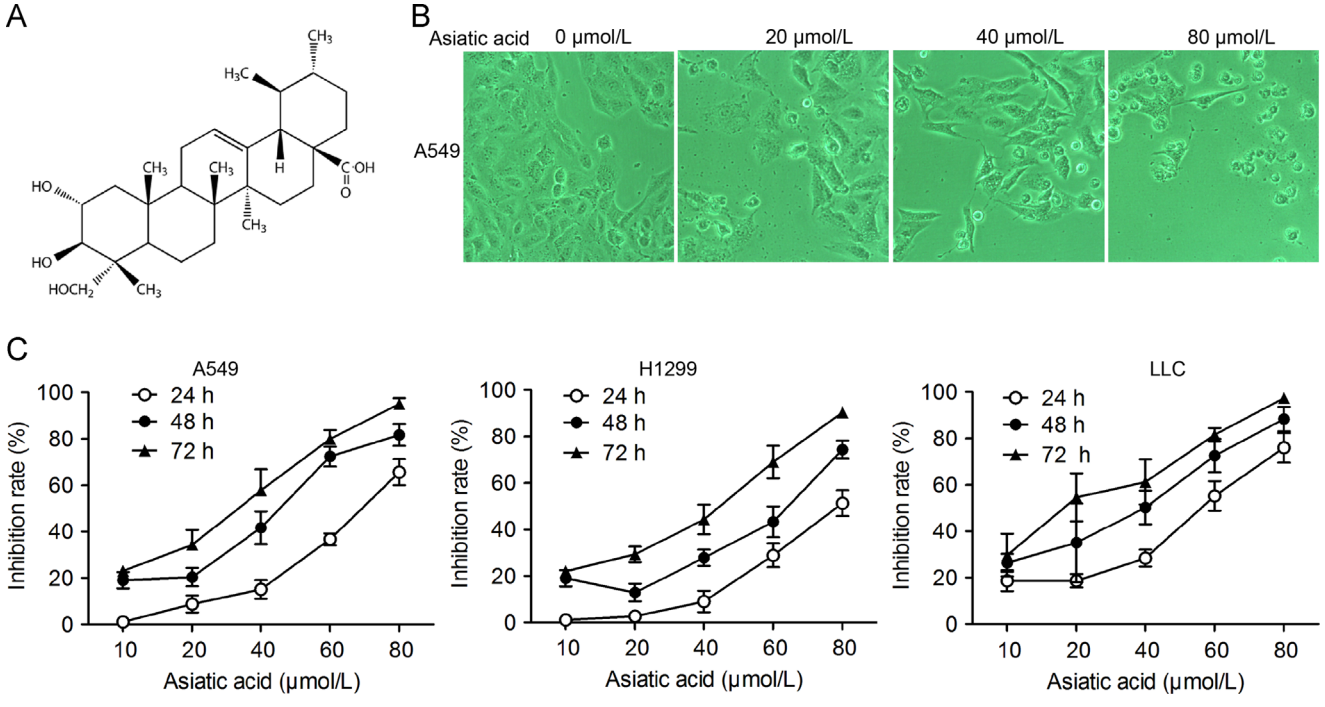

Figure 1 Asiatic acid inhibits lung cancer cell proliferation. (A) Structure of asiatic acid; (B) and (C) A549, H1299 and LLC cells exposed to various concentrations of asiatic acid. (B) Photographs showing morphological changes in cells; (C) Cell proliferation determined by the MTT assay every 24 h. Data represent mean ± SD of three different experiments.

shaped control cells, AA-treated cells lost their adherent phenotype and assumed a circular morphology.

3.2. *Apoptosis*

A549 cells treated with AA for 24 h and then stained with DAPI showed that nuclei became condensed and divided into several parts with the emergence of apoptotic bodies (Fig. 2A). Other treated cells stained with annexin V/PI showed the number of annexin V^+cells was markedly increased from 17.1% to 54.5% (at 40 μmol/L) and to 63.9% (at 80 μmol/L). To determine the involvement of the caspase cascade in AA-induced apoptosis, the expression of caspases was examined by Western blot. It was found that the hallmarks of apoptosis (PARP, caspase-9 and caspase-3) were activated/cleaved in A549 cells treated with AA in a dose- and time-dependent manner (Fig. 3A and B). In addition, cytochrome *c* was transferred from the mitochondrial intermembrane to the cytoplasm (Fig. 3C). These results support the view that AA induces significant apoptosis in A549 cells.

3.3. *Mitochondrial dysfunction*

As mitochondria are critical for apoptosis, it was logical to explore the effect of AA on mitochondrial function. Using JC-1 to evaluate the mitochondrial membrane potential, it was found that treatment with 20, 40, and 80 μmol/L AA for 12 h led to mitochondrial membrane potential collapse as shown by enhanced green intensity, reduced red

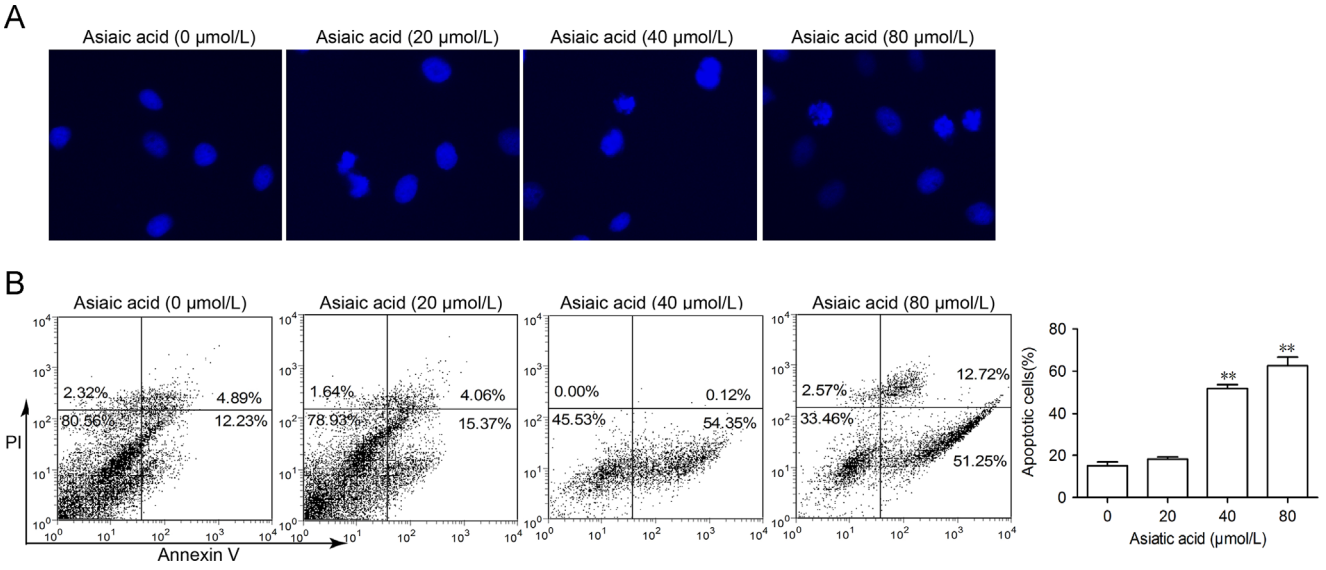

Figure 2 Asiatic acid induces apoptotic cell death and cell cycle arrest in lung cancer cells. (A) A549 cells were treated with asiatic acid (20, 40 and 80 μmol/L) for 24 h, stained with DAPI and nuclei photographed. (B) A549 cells treated with asiatic acid were collected and subjected to annexin V/PI analysis (B). Data represent mean ± SEM of three different experiments.

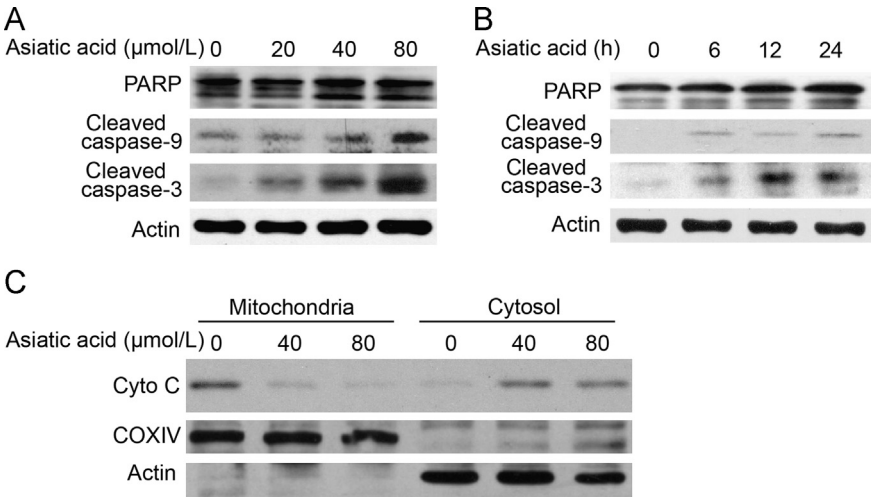

Figure 3 Asiatic acid induces apoptotic cell death *via* a mitochondrial pathway. (A) and (B) A549 cells were exposed to asiatic acid (80 μmol/L for 3, 6, 12, 24 h or 20, 40, 80 μmol/L for 12 h) after which PARP, caspase-9 and caspase-3 activation was assessed by Western blot. (C) The release level of cytochrome *c* from mitochondria was examined by Western blotting.

intensity (Fig. 4A) and reduced red/green ratio in a dose- and time-dependent manner (Fig. 4B and C). Intracellular ROS was then assessed by DCFH-DA florescence and found to be significantly elevated by AA treatment again in a dose- and time-dependant manner. To determine the role of ROS in AA-induced apoptosis, we investigated whether inhibition of ROS by NAC affected A549 cell death. As shown in Fig. 4F, the MTT assay revealed that apoptosis induced by AA was markedly reduced by NAC. Thus the results indicate that AA triggers mitochondrial dysfunction and ROS-dependent cell death in A549 cells.

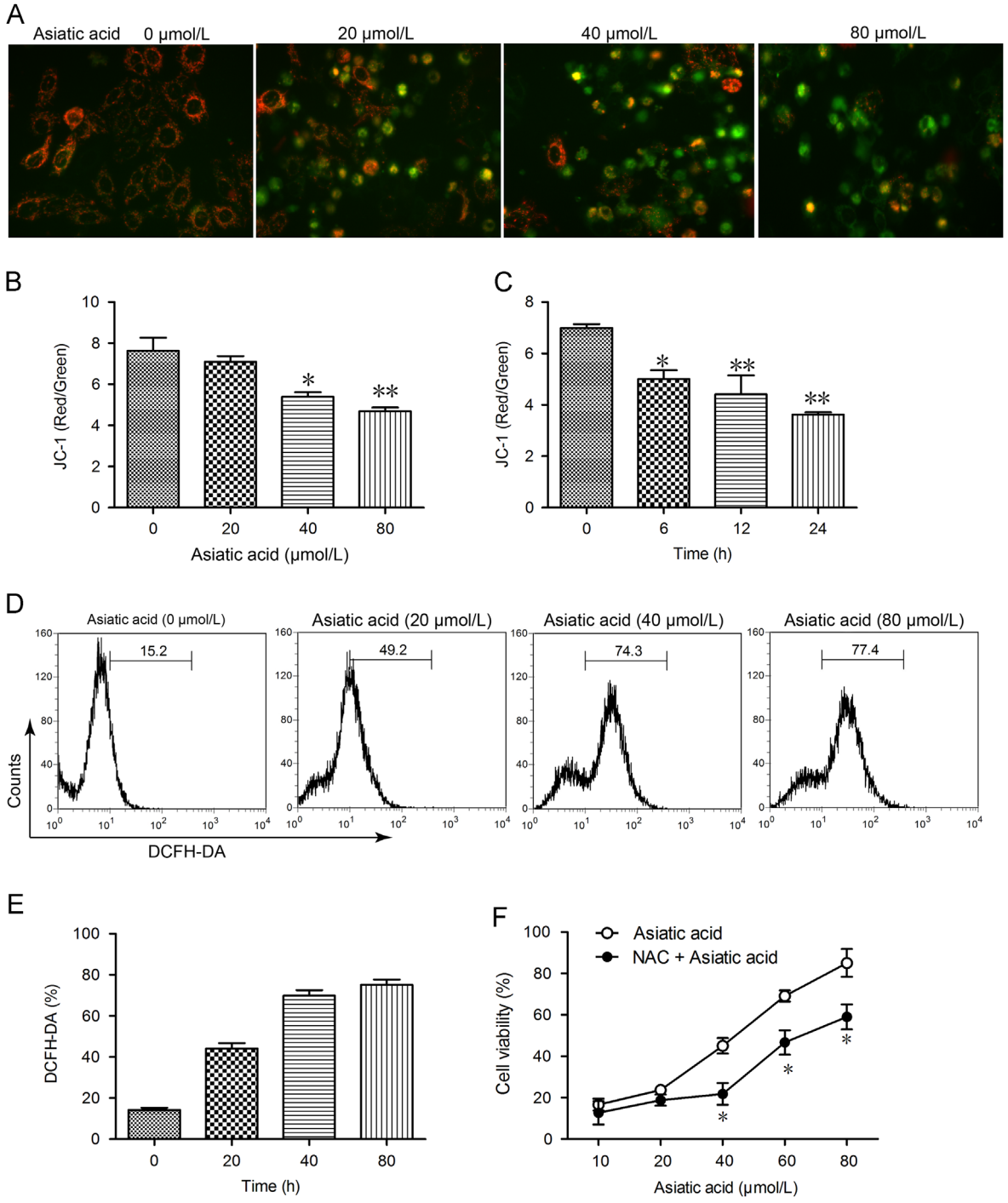

Figure 4 Asiatic acid treatment causes mitochondrial dysfunction. (A)–(C) A549 cells were exposed to asiatic acid (80 μmol/L for 3, 6, 12, 24 h or 20, 40, 80 μmol/L for 12 h) and the mitochondrial membrane potential (JC-1 staining, red/green fluorescence ratio) photographed by fluorescence microscopy and quantified by fluorescence spectrometry. (D) and (E) A549 cells were exposed to asiatic acid (20, 40, 80 μmol/L for 12 h) and the level of ROS detected by DCFH-DA staining. (F) A549 cells were exposed to asiatic acid (20, 40 and 80 μmol/L for 12 h) with or without NAC (2.5 mmol/L) for 48 h. The MTT assay was used to evaluate cell viability. Data represent mean ± SD of three different experiments. $^{*}P<0.05$, $^{**}P<0.01$ *vs.* control.

3.4. *AA-induced protective autophagy*

As mitochondrial damage is also critical for autophagy, it was appropriate to examine whether autophagic cell death contributes to the cytotoxic effects of AA. This possibility was analyzed by seeking evidence that LC3-I (19 kD) is converted to the preautophagosomal and autophagosomal membrane-bound form of LC3-II (17 kD) (a specific marker for autophagosome formation). As shown in Fig. 5, the formation of LC3-labeled vacuoles was markedly increased in A549 cells after treatment with 80 μmol/L AA for 12 h. LC3-I to LC3-II conversion markedly increased with time and concentration of AA as shown by Western blot (Fig. 5A and B).

To establish whether autophagy is associated with cell death, the effect of autophagy inhibitors was examined. It was found using the MTT assay that pretreatment with the autophagy inhibitor 3-MA or the autophagolysosome fusion inhibitor CQ

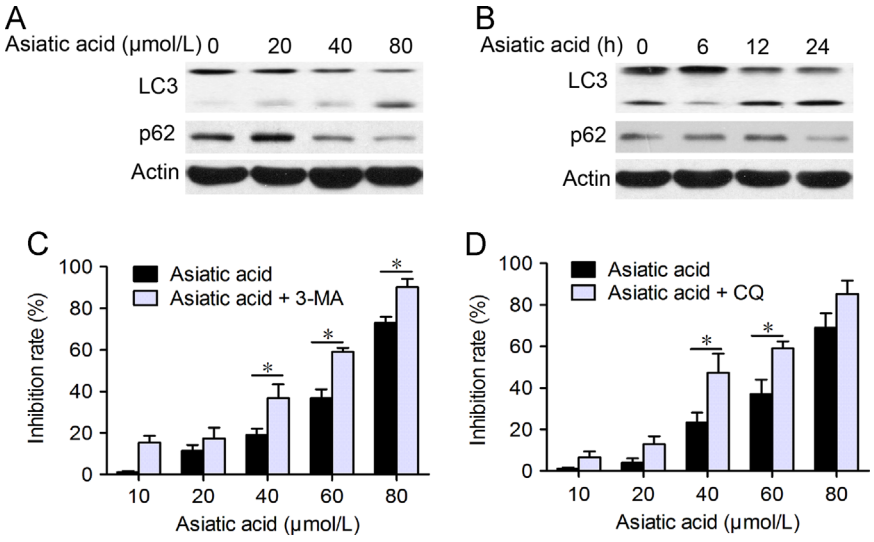

Figure 5 Asiatic acid induces cell protective autophagy. (A) and (B) A549 cells were treated with asiatic acid (20, 40, 80 μmol/L for 12 h or 80 μmol/L for 6, 12, 24 h) and protein expression of LC3 and p62 analyzed by Western blot. (C) and (D) A549 cells were treated with various concentrations of asiatic acid for 24 h with or without 3-MA and CQ pretreatment (2 h). The MTT assay was used to evaluate cell viability. Data are mean ± SD of three different experiments. $^{*}P<0.05$, $^{**}P<0.01$ *vs.* indicated.

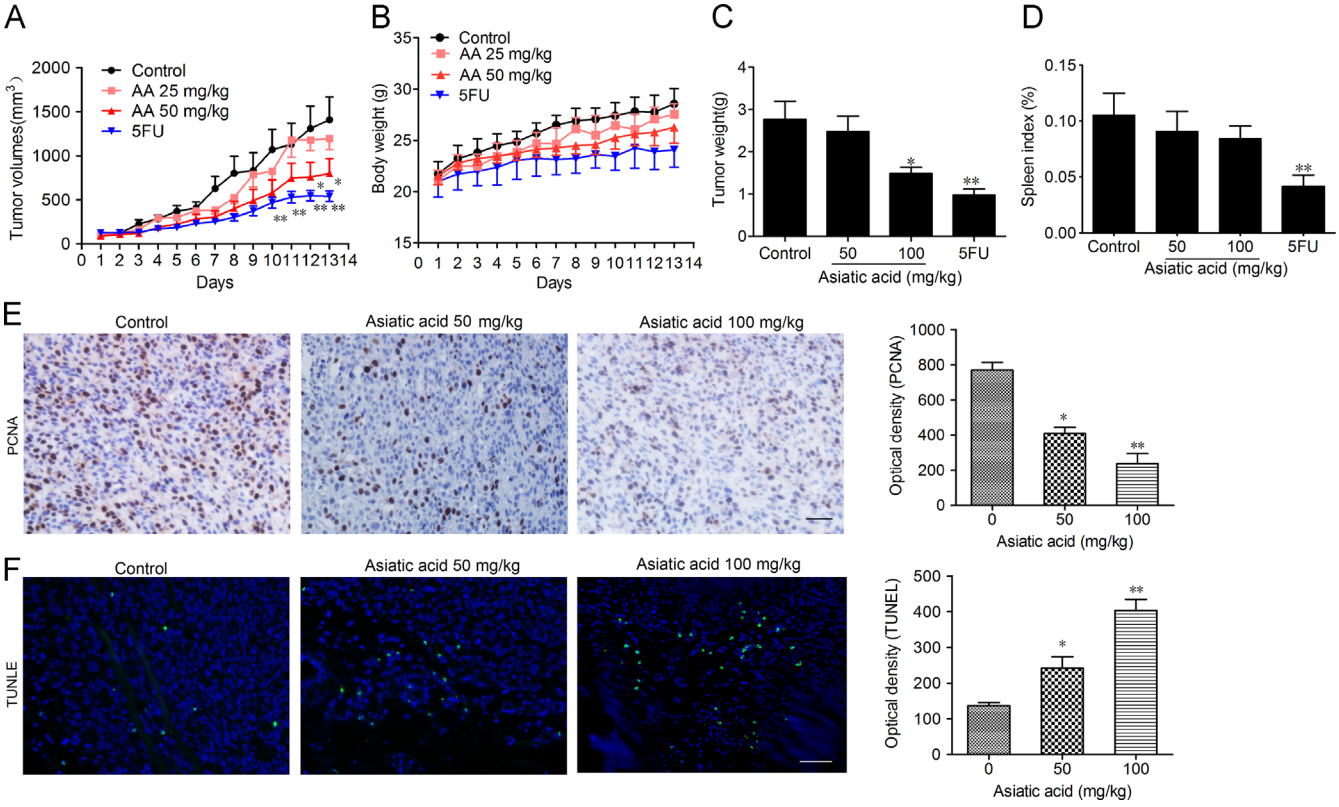

Figure 6 Asiatic acid inhibits tumor growth *in vivo*. 1×10^6 LLC cells were transplanted subcutaneously into the armpit of the C57 mice. Three days after transplantation, mice were randomly allocated to either control or treatment groups ($n=6$). Drugs were administered i.g. on days 1–13. (A) and (B) Tumor volume and mouse bodyweight were recorded daily. After sacrifice, solid tumors were separated and weighed. (C) and (D) The spleen index was calculated. (E) Paraffin sections of tumor tissues from mice were analyzed by H&E staining and TUNEL staining and (F) optical density was calculated. Scale bar, 50 μm. Data represent mean ± SEM, $n=8$, $^{*}P<0.05$, $^{**}P<0.01$ *vs.* control.

significantly prevented AA-induced cell death in a dose-dependent manner (Fig. 5C and D). These results support the premise that autophagy protects A549 cells from AA-induced cell death.

3.5. *In vivo anticancer activity*

In the mouse xenograft model of LLC cells in C57BL/6J mice, once daily administration of AA (50 and 100 mg/kg) inhibited tumor growth in a dose-dependent manner (Fig. 6A and C). The tumor inhibition rate at 100 mg/kg was 54%. 5-Fluorouracil (5FU) significantly reduced the bodyweight and spleen index in mice whereas no significant change was observed in AA-treated mice (Fig. 6B and D). According to *ex vivo* results, both the TUNEL assay and PCNA staining of tumor tissue from mice proved that proliferation of tumor cells was inhibited and that tumor cells were undergoing significant apoptosis after AA treatment (Fig. 6E and F). In summary, the results show that AA can effectively suppress tumor growth *in vivo* with no significant side effects.

4. Discussion

In the present study, we evaluated the effects of AA on lung cancer cell lines and clarified the mechanism of these effects. Our results show that AA is able to inhibit cell proliferation and cause cell death both *in vitro* and *in vivo*. In addition, we confirmed that AA can induce apoptosis mainly through interference with the mitochondrial membrane potential which stimulates the release of cytochrome *c* and triggers caspase signaling pathways and PARP activation which in turn lead to apoptotic cell death.

It is well established that mitochondria and ROS play a central role in the process of cell death, including apoptosis and autophagy[16–18]. Under excessive oxidative stress, the accumulation of ROS reaches a threshold level which triggers the opening of mitochondrial permeability transition pores (MPTPs) or oxidation of mitochondrial outer membranes. This in turn leads to the simultaneous collapse of the mitochondrial membrane potential ($\Delta\Psi_m$) and a transient increase in ROS generation by the respiratory chains that transform O_2 to ATP[19,20]. With the increase in mitochondrial permeability, the released proteins and ROS play many roles in cellular processes including DNA damage, activation of signaling pathways and activation of transcription factors leading to upregulation of genes[21]. Consistent with these observations, AA induces mitochondrial dysfunction including matrix metalloproteinase (MMP) collapse subsequent to ROS accumulation (Fig. 4).

Apoptosis type I is characterized by nuclear condensation and fragmentation, apoptotic body emergence without plasma membrane breakdown. During apoptosis, many death signals converge on mitochondria, especially the release of cytochrome *c* due to the increased permeability of the outer mitochondrial membrane and, coordinately, the activation of downstream caspase signaling[22]. We observed AA-induced activations of PARP, caspase-9 and caspase-3 and the disruption of the mitochondrial membrane potential indicating that mitochondria are involved in AA-induced cell death (Figs. 2 and 3).

As type II cell death, autophagy may play an important role in cancer cell death induced by chemotherapy. Autophagy is a dynamic process involving autophagic flux whereby autophagosomes are stimulated to form, engulf cellular contents, fuse with lysosomes and bring about the degradation of the contents[23]. Autophagy has both a positive and negative face. On one hand, it is seen as a physiological process that plays a protective role when cells encounter environmental stress such as starvation or pathogen infection[24]. On the other hand, excess autophagy can act as a pro-death mechanism[25]. In A549 cells, AA treatment led to elevation of the ratio of LC3-II to LC3-I indicating the occurrence of autophagy. In addition, when combined with autophagy inhibitors such as 3-MA and CQ, AA-induced cell death was elevated. These results suggest that autophagy plays a protective role during AA treatment (Fig. 5) as it does during exposure to many other chemicals[26–29]. In this situation, suppression of this protective autophagy is important to potentiate chemotherapies[30].

In conclusion, the present study provides further evidence that AA is a promising anticancer agent with the ability to induce apoptosis mainly through a mitochondrion-mediated pathway. Thus AA alone or in combination with autophagy inhibitors or chemotherapeutic agents may represent a new option in the treatment of lung cancer.

References

1. Siegel RL, Miller KD, Jemal A. Cancer statistics, 2015. *CA Cancer J Clin* 2015;**65**:5–29.
2. Minguet J, Smith KH, Bramlage P. Targeted therapies for treatment of non-small cell lung cancer—recent advances and future perspectives. *Int J Cancer* 2016;**138**:2549–61.
3. Landi L, Cappuzzo F. Experience with erlotinib in the treatment of non-small cell lung cancer. *Ther Adv Respir Dis* 2015;**9**:146–63.
4. Schiller GJ, O'Brien SM, Pigneux A, Deangelo DJ, Vey N, Kell J, et al. Single-agent laromustine, a novel alkylating agent, has significant activity in older patients with previously untreated poor-risk acute myeloid leukemia. *J Clin Oncol* 2010;**28**:815–21.
5. Sharma SV, Bell DW, Settleman J, Haber DA. Epidermal growth factor receptor mutations in lung cancer. *Nat Rev Cancer* 2007;**7**:169–81.
6. Pérez-Soler R, Chachoua A, Hammond LA, Rowinsky EK, Huberman M, Karp D, et al. Determinants of tumor response and survival with erlotinib in patients with non-small-cell lung cancer. *J Clin Oncol* 2004;**22**:3238–47.
7. Ciardiello F, Tortora G. EGFR antagonists in cancer treatment. *N Engl J Med* 2008;**358**:1160–74.
8. Xiong YY, Ding HQ, Xu MF, Gao J. Protective effects of asiatic acid on rotenone- or H_2O_2-induced injury in SH-SY5Y cells. *Neurochem Res* 2009;**34**:746–54.
9. Shetty BS, Udupa SL, Udupa AL, Somayaji SN. Effect of *Centella asiatica* L (Umbelliferae) on normal and dexamethasone-suppressed wound healing in Wistar Albino rats. *Int J Low Extrem Wounds* 2006;**5**:137–43.
10. Guo WJ, Liu W, Jin B, Geng J, Li J, Ding HQ, et al. Asiatic acid ameliorates dextran sulfate sodium-induced murine experimental colitis *via* suppressing mitochondria-mediated NLRP3 inflammasome activation. *Int Immunopharmacol* 2015;**24**:232–8.
11. Guo WJ, Liu W, Hong SC, Liu HL, Qian C, Shen Y, et al. Mitochondria-dependent apoptosis of Con A–activated T lymphocytes induced by asiatic acid for preventing murine fulminant hepatitis. *PLoS One* 2012;**7**:e46018.
12. Park BC, Bosire KO, Lee ES, Lee YS, Kim JA. Asiatic acid induces apoptosis in SK-MEL-2 human melanoma cells. *Cancer Lett* 2005;**218**:81–90.
13. Lee YS, Jin DQ, Kwon EJ, Park SH, Lee ES, Jeong TC, et al. Asiatic acid, a triterpene, induces apoptosis through intracellular Ca^{2+} release and enhanced expression of p53 in HepG2 human hepatoma cells. *Cancer Lett* 2002;**186**:83–91.
14. Hsu YL, Kuo PL, Lin LT, Lin CC. Asiatic acid, a triterpene, induces apoptosis and cell cycle arrest through activation of extracellular signal-regulated kinase and p38 mitogen-activated protein kinase pathways in human breast cancer cells. *J Pharmacol Exp Ther* 2005;**313**:333–44.
15. Park BC, Paek SH, Lee YS, Kim SJ, Lee ES, Choi HG, et al. Inhibitory effects of asiatic acid on 7,12-dimethylbenz[*a*]anthracene

and 12-*O*-tetradecanoylphorbol 13-acetate-induced tumor promotion in mice. *Biol Pharm Bull* 2007;**30**:176–9.
16. Wu CC, Bratton SB. Regulation of the intrinsic apoptosis pathway by reactive oxygen species. *Antioxid Redox Signal* 2013;**19**:546–58.
17. Dan Dunn J, Alvarez LAJ, Zhang XZ, Soldati T. Reactive oxygen species and mitochondria: a nexus of cellular homeostasis. *Redox Biol* 2015;**6**:472–85.
18. Green DR, Llambi F. Cell death signaling. *Cold Spring Harb Perspect Biol* 2015;**7**:a006080.
19. Nickel A, Kohlhaas M, Maack C. Mitochondrial reactive oxygen species production and elimination. *J Mol Cell Cardiol* 2014;**73**:26–33.
20. Zorov DB, Juhaszova M, Sollott SJ. Mitochondrial reactive oxygen species (ROS) and ROS-induced ROS release. *Physiol Rev* 2014;**94**:909–50.
21. Sabharwal SS, Schumacker PT. Mitochondrial ROS in cancer: initiators, amplifiers or an Achilles' heel?. *Nat Rev Cancer* 2014;**14**:709–21.
22. Desagher S, Martinou JC. Mitochondria as the central control point of apoptosis. *Trends Cell Biol* 2000;**10**:369–77.
23. Thorburn A. Autophagy and its effects: making sense of double-edged swords. *PLoS Biol* 2014;**12**:e1001967.
24. Klionsky DJ, Emr SD. Autophagy as a regulated pathway of cellular degradation. *Science* 2000;**290**:1717–21.
25. Galluzzi L, Maiuri MC, Vitale I, Zischka H, Castedo M, Zitvogel L, et al. Cell death modalities: classification and pathophysiological implications. *Cell Death Differ* 2007;**14**:1237–43.
26. Tang MC, Wu MY, Hwang MH, Chang YT, Huang HJ, Lin AM, et al. Chloroquine enhances gefitinib cytotoxicity in gefitinib-resistant non-small cell lung cancer cells. *PLoS One* 2015;**10**:e0119135.
27. Yu L, Gu CP, Zhong DS, Shi LL, Kong Y, Zhou ZT, et al. Induction of autophagy counteracts the anticancer effect of cisplatin in human esophageal cancer cells with acquired drug resistance. *Cancer Lett* 2014;**355**:34–45.
28. Zhao XG, Sun RJ, Yang XY, Liu DY, Lei DP, Jin T, et al. Chloroquine-enhanced efficacy of cisplatin in the treatment of hypopharyngeal carcinoma in xenograft mice. *PLoS One* 2015;**10**:e0126147.
29. Pan XH, Zhang XL, Sun HL, Zhang JJ, Yan MM, Zhang HB. Autophagy inhibition promotes 5-fluorouraci-induced apoptosis by stimulating ROS formation in human non-small cell lung cancer A549 cells. *PLoS One* 2013;**8**:e56679.
30. Pascolo S. Time to use a dose of chloroquine as an adjuvant to anti-cancer chemotherapies. *Eur J Pharmacol* 2016;**771**:139–44.